Zoological Journal of the Linnean Society, 2018, **XX**, 1–14. With 5 figures.

Solving a thorny situation: DNA and morphology illuminate the evolution of the leaf beetle tribe Dorynotini (Coleoptera: Chrysomelidae: Cassidinae)

MARIANNA V. P. SIMÕES[1,*], STEPHEN M. BACA[2], EMMANUEL F. A. TOUSSAINT[3], DONALD M. WINDSOR[4] and ANDREW E. Z. SHORT[2]

[1]*Department of Marine Zoology-Crustaceans, Senckenberg Research Institute and Natural History Museum, Senckenberganlage 25, 60325 Frankfurt am Main, Germany*
[2]*Department of Ecology and Evolutionary Biology; and Division of Entomology, Biodiversity Institute, University of Kansas, Lawrence, KS 66045, USA*
[3]*Florida Museum of Natural History, University of Florida, Powell Hall, 3215 Hull Road, Gainesville, FL 32611–2710, USA*
[4]*Smithsonian Tropical Research Institute, Apartado 0843-03092, Balboa, Ancon, Republica de Panamá*

Received 7 March 2018; revised 28 June 2018; accepted for publication 10 September 2018

The Neotropical tribe Dorynotini is characterized by a conspicuous tubercle or spine adorning the elytra, which, along with a few other characters, has been used to differentiate its recognized five genera and two subgenera. However, relationships among these taxa and the evolutionary origin of the pronounced tubercle remain speculative. Here we present the first total-evidence phylogenetic reconstruction of Dorynotini to investigate the homology and evolution of the elytral tubercle. Our analyses are based on 89 discrete morphological characters and DNA sequence data from three gene regions. Phylogenetic relationships were inferred using Bayesian inference, maximum likelihood and maximum parsimony. Our analyses support the respective monophyly of Dorynotini and its genera and subgenera, except the paraphyletic *Dorynota s.s*. Species endemic to the Greater Antilles form a clade with three distinct morphotypes. ***Omoteina aculeata*** (Boheman, 1854) **nov. comb.** is transferred from the genus *Dorynota*, and ***Paratrikona*** Spaeth, 1923 **nov. syn.** is found to be congeneric with *Omoteina* Chevrolat, 1836. The spiniform projection is found to be plesiomorphic within Dorynotini and convergently reduced/lost in different lineages of the tribe. Some morphological characters defining dorynotine taxa are homoplastic, requiring re-evaluation guided by molecular analyses for more accurate classification and an improved understanding of taxon evolution.

ADDITIONAL KEYWORDS: ancestral character reconstructionn – Caribbean – Insecta – insect phylogeny – molecular systematics – Neotropical – phylogenetic systematics – phylogenetics, Bayesian analysis – phylogenetics, maximum likelihood – taxa, new classification – taxonomy – total-evidence phylogenetic reconstruction.

INTRODUCTION

Cassidinae *s.l.*, commonly known as tortoise beetles, is the second largest subfamily of leaf beetles, with ~6300 described species worldwide (Borowiec & Świętojańska, 2018). The tribe Dorynotini Monrós & Viana, 1949 is an exclusively Neotropical clade of cassidines (Chaboo, 2007) distributed from central Mexico to northern Argentina, including the Greater Antilles (Borowiec & Świętojańska, 2018). The tribe currently contains 56 species distributed in five genera: *Dorynota* Chevrolat, 1836, *Heteronychocassis* Spaeth, 1915 (one species), *Omoteina* Chevrolat, 1836 (one species), *Paranota* Monrós & Viana, 1949 (five species) and *Paratrikona* Spaeth, 1923 (seven species). The most diverse genus, *Dorynota*, is further split into two subgenera: *Dorynota s.s.* (18 species) and *Akantaka* Maulik, 1916 (24 species) (Bouchard *et al.*, 2011; Simões, 2014; Simões & Sekerka, 2014; Simões & Sekerka, 2015; Borowiec & Świętojańska, 2018).

Chevrolat (in Dejean, 1836) first proposed the genus *Dorynota* for Neotropical cassidines with a

*Corresponding author. E-mail: mariannavpsimoes@gmail.com

post-scutellar spiniform projection. Later, Maulik (1916) erected two additional genera, *Akantaka* and *Trikona*, based on the presence and shape of the post-scutellar projection on the elytra and provided an identification key, where the shape of the scutellum was also proposed to distinguish the three genera. Monrós & Viana (1949) considered the classification proposed by Chapuis (1835) as better supported by morphological characters, and revalidated the tribe (= group; Chapuis, 1835) 'Batonotites', changing its name to Dorynotini, characterized by: (1) the presence of insertion pockets (for the posterior margin of the pronotum) on the anterior margin of the elytra; (2) the presence and shape of a vertical post-scutellar spine/tubercle on the elytral suture; and (3) the symmetry and angle between pretarsal claws. The genera in this tribe were grouped mostly based on the presence or absence and shape of the elytral spine/tubercle, forming five conspicuous, recognizable morphotypes (Figs 1, 2). Moreover, Monrós & Viana (1949) described the genus *Paranota* and recognized six other genera in the tribe: *Akantaka*, *Dorynota*, *Heteronychocassis*, *Omoteina*, *Paratrikona* and *Eremionycha* Spaeth, 1911.

Hincks (1952) downgraded *Akantaka* to a subgenus of *Dorynota* and synonymized the genus *Trikona* with *Omoteina* for sharing the type species (*Cassida humeralis* Olivier, 1808), a classification that was accepted in later works (Borowiec, 1999; Borowiec & Świętojańska, 2018). In 1999, Borowiec transferred *Eremionycha* to the tribe Cassidini Gyllenhal, resulting in the current composition of Dorynotini.

Multiple cladistic analyses based on adult morphology (Borowiec, 1995; Chaboo, 2007; López-Pérez *et al.*, 2017) and molecular data (12S mitochondrial DNA; Hsiao & Windsor, 1999) have supported the monophyly of the Dorynotini. However, phylogenetic relationships among genera remain unresolved, and insights about the homology and function of the elytral spine/tubercle are still lacking.

Spaeth (1923) observed that members of the tribe lacking the post-scutellar projection or with a tubercle-shaped projection are restricted to the Greater Antilles (*Omoteina* and *Paratrikona*) and the Amazon Basin region (*Akantaka*), whereas species with a spiniform post-scutellar projection occur throughout the Neotropics, with their diversity concentrated in the southern part of the tribal range. Based on this distribution pattern, he suggested that the presence and prominence of the post-scutellar projection would be correlated with environmental gradients across the distribution of the clade, allowing the species with the spine to invade cooler areas of the Neotropics. Simões *et al.* (2017) rejected the hypothesis posed by Spaeth

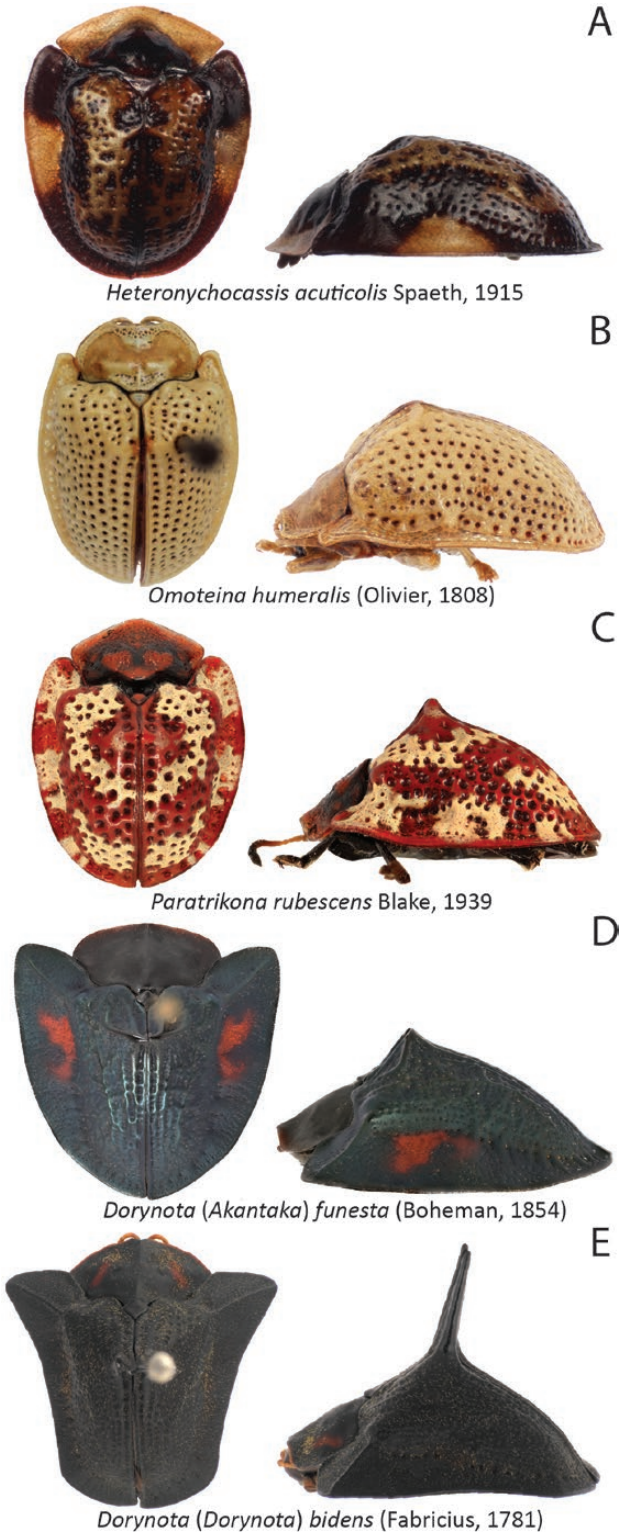

Figure 1. A–E, dorsal and lateral habitus of the five morphotypes found within the tribe Dorynotini.

Figure 2. A–C, adult Dorynotini. A, male and female of *Dorynota* (*s.s.*) *pugionata* (Germar) copulating. B, *Omoteina humeralis* (Olivier). C, *Dorynota* (*Akantaka*) *funesta* (Boheman). [Phototographs: A, Victor Chaves Machado; C, alapi973 (Flickr: https://www.flickr.com/people/83287919@N00/)].

(1923), concluding that morphological divergence occurs with high levels of environmental overlap, and suggested that the presence of the post-scutellar projection could be related to biotic interactions, perhaps as camouflage to guard against predation.

The tribe Dorynotini was last reviewed by Monrós & Viana (1949), and no systematic work has been conducted at the tribal level since. Here, we combine morphological and molecular data to (1) test the monophyly of the tribe; (2) test the monophyly and relationships among the genera within the tribe; (3) elucidate biogeographical patterns; and (4) investigate the homology and evolution of the post-scutellar projection and other key characters using ancestral character state reconstruction (ACSR). This is the first systematic attempt to resolve relationships among dorynotine lineages, allowing further insight into their intriguing evolution and morphology.

MATERIAL AND METHODS

Taxon sampling

For morphological and molecular datasets, we sampled 16 species of Dorynotini, including four of the five genera and both subgenera (Supporting Information, Table S1). We were unable to include the monotypic genus *Heteronychocassis*, from French Guiana. The species is known only from the heavily damaged holotype, deposited at The Manchester Museum (Simões & Sekerka, 2014). Although sampling of in-group species is limited, we sought to cover the diversity of genera within the tribe, in which species are extremely rare in the field and in collections, usually known only from short series of specimens (Blake, 1939; Borowiec, 2009; Simões, 2017).

We sampled a broad selection of outgroup taxa because the relationships among tribes of Cassidinae remain contentious (Borowiec, 1995; Hsiao & Windsor, 1999; Chaboo, 2007). We sampled 15 species representing the tribes that had been recovered in past studies as closely related to Dorynotini, Cassidini Gyllenhal, 1813, Ischyrosonychini Chapuis, 1875 and Mesomphaliini Chapuis, 1875 (Borowiec, 1995; Hsiao & Windsor, 1999; Chaboo, 2007; Lopez et al., 2017) (Table 1). Specimens for sequencing were obtained during fieldwork in Bolivia, Brazil, the Dominican Republic, French Guiana and Panama.

Morphological characters

Eighty-nine phylogenetically informative adult morphological characters were used to assess interspecific morphological differences and build a discrete data matrix (Supporting Information, Appendix S1 and Table S2). They include 85 external anatomical characters and four internal anatomical characters (Supporting Information, Appendix S1).

To prepare for the morphological examinations of the exo- and endoskeleton including wings, specimens were placed in a heated aqueous solution of 10% potassium hydroxide (KOH) for 7 min. Structural terminology follows Monrós & Viana (1949), Borowiec (2005) and Chaboo (2007), with the following exceptions: hind wing venation, which follows Suzuki (1994); and the metendosternite, which follows Crowson (1938) and Hübler & Klass (2013). All character states were treated as unordered in all analyses. Missing characters states were scored as '?'.

Extraction of DNA and gene sequencing

Total genomic DNA was extracted from legs or thoracic tissue of specimens preserved in 96% ethanol using a Qiagen DNeasy extraction kit (Qiagen, Valencia, CA,

Table 1. List of specimens used in this study

Tribe	Genus	Species	Code	Locality	*CO1*	*CAD*	28S
Cassidini	*Coptocycla*	*arcuata*	MVPS32B	Brazil, Rio de Janeiro	MH717727	MH717755	MH744688
Cassidini	*Charidotella*	*quadrisignata*	MVPS22B	Dominican Republic, Santo Domingo	MH717726	MH717754	MH744687
Cassidini	*Deloyala*	*fuliginosa*	MVPS28B	Dominican Republic, Santo Domingo	MH717729	MH717757	MH744690
Cassidini	*Eremionycha*	*bahiana*	MVPS13B	Brazil, Rio de Janeiro	MH717740	MH717767	MH744702
Cassidini	*Metriona*	*elatior*	MVPS08B	Brazil, Rio de Janeiro	MH717742	MH717770	MH744705
Cassidini	*Plagiometriona*	*ambigena*	MVPS35B	Brazil, Rio de Janeiro	MH717750	MH717779	MH744714
Cassidini	*Plagiometriona*	*inscripta*	MVPS23B	Brazil, Rio de Janeiro	MH717749	MH717778	MH744713
Cassidini	*Syngambria*	*bisinuata*	MVPS31B	Brazil, Minas Gerais	MH717753	MH717782	MH744717
Dorynotini	*Dorynota*	*pugionata*	MVPS09B	Brazil, Minas Gerais	MH717730	MH717758	MH744691
Dorynotini	*Dorynota*	*aculeata*	MVPS17B	Dominican Republic, Barahona	MH717731	MH717759	MH744692
Dorynotini	*Dorynota*	*bidens*	MVPS16B	Brazil, Rio de Janeiro	MH717732	MH717760	MH744693
Dorynotini	*Dorynota*	*boliviana*	MVPS01B	Bolivia, Andres Ibanez	MH717733	MH717761	MH744694
Dorynotini	*Dorynota*	*collucens*	MVPS05B	Bolivia, Florida	MH717734	MH717762	MH744695
Dorynotini	*Dorynota*	*distincta*	MVPS11B	Panama	MH717735	MH717763	MH744696
Dorynotini	*Dorynota*	*funesta*	DW7829	French Guiana, Patawa	–	–	MH744697
Dorynotini	*Dorynota*	*insidiosa*	MVPS04B	Panama, Chiriqui	MH717736	MH717764	MH744698
Dorynotini	*Dorynota*	*monoceros*	DW0515	Brazil, Colombo	MH717737	–	MH744699
Dorynotini	*Dorynota*	*parallela*	MVPS20B	Brazil, Minas Gerais	MH717738	MH717765	MH744700
Dorynotini	*Dorynota*	*truncata*	MVPS06B	French Guiana	MH717739	MH717766	MH744701
Dorynotini	*Omoteina*	*humeralis*	MVPS18B	Dominican Republic, Barahona	MH717743	MH717771	MH744706
Dorynotini	*Paranota*	*minima*	MVPS07B	Bolivia, Andres Ibanez	MH717744	MH717772	MH744707
Dorynotini	*Paranota*	*rugosa*	MVPS14B	Brazil, Mato Grosso	MH717745	MH717773	MH744708
Dorynotini	*Paranota*	*spinosa*	MVPS15B	Brazil, Mato Grosso	–	MH717774	MH744709
Dorynotini	*Paratrikona*	*rubescens*	MVPS19B	Brazil, Mato Grosso	MH717746	MH717775	MH744710
Mesomphaliini	*Cyrtonota*	*sexpustulata*	MVPS41B	Brazil, Rio de Janeiro	MH717728	MH717756	MH744689
Mesomphaliini	*Mesomphalia*	*variolaris*	MVPS46B	Brazil, Bahia	–	MH717769	MH744704
Mesomphaliini	*Stolas*	*conspersa*	MVPS44B	Brazil, Rio de Janeiro	MH717751	MH717780	MH744715
Mesomphaliini	*Stolas*	*modica*	MVPS43B	Brazil, Rio de Janeiro	MH717752	MH717781	MH744716
Physonotini	*Eurypepla*	*calachoroa*	MVPS56B	USA, Florida	MH717741	MH717768	MH744703
Physonotini	*Physonota*	*attenuata*	MVPS53B	Nicaragua, Granada	MH717747	MH717776	MH744711
Physonotini	*Physonota*	*gigantea*	MVPS52B	Nicaragua, Granada	MH717748	MH717777	MH744712

Classification follows Borowiec & Świetojańska (2018). GenBank accession codes for each successfully sequenced or downloaded gene fragment will be provided once the paper is accepted.

Table 2. List of primers used to amplify the gene fragments used in this study

Gene	Location	Primer	Direction	Sequence	Reference
CO1	Mitochondrial	Jerry	Forward	CAACAYTTATTTTGATTTTTTGG	Simon *et al.* (1994)
CO1	Mitochondrial	Pat	Reverse	ATCCATTACATATAATCTGCCATA	Simon *et al.* (1994)
28S	Nuclear	NLF184-21	Forward	ACCCGCTGAAYTTAAGCATAT	Van der Auwera *et al.* (1994)
28S	Nuclear	LS1041R	Reverse	TACGGACRTCCATCAGGGTTTCCCCTGACTTC	Wild & Maddison (2008)
CAD	Nuclear	CD439F	Forward	TTCAGTGTACARTTYCAYCCHGARCAYAC	Wild & Maddison (2008)
CAD	Nuclear	CD688R	Reverse	TGTATACCTAGAGGATCDACRTTYTCCATRTTRCA	Wild & Maddison (2008)

USA). We used the primers listed in Table 2 to amplify and sequence one mitochondrial gene fragment, cytochrome oxidase subunit 1 (*CO1*, 588 bp), and two nuclear gene fragments, 28S (995 bp) and carbamoylphosphate synthetase (*CAD*, 723 bp).

Polymerase chain reactions (PCRs) consisted of the following cycling steps: initial denaturation for 4 min at 95–98 °C; 30–40 cycles of denaturation for 30 s at 95–98 °C, annealing for 30 s at different temperatures depending on the primer pair (see below), and extension for 1–1.5 min at 72 °C; with a final extension for 5–10 min at 72 °C. The annealing temperatures for each gene fragment were as follows: 50–51 °C for *CO1* (Baca *et al.*, 2017) and 50 °C for 28S. Fragment 1 of *CAD* was generated using a 'touchdown' PCR with the following conditions: initial denaturation at 95 °C (3.5 min); six cycles of 95 °C (30 s), 50 °C (30 s) and 72 °C (1 min); ten cycles of 95 °C (30 s), 51 °C (30 s) and 72 °C (1 min); ten cycles of 95 °C (30 s), 52 °C (30 s) and 72 °C (1 min); six cycles of 95 °C (30 s), 53 °C (30 s) and 72 °C (1 min); four cycles of 95 °C (30 s), 54 °C (30 s) and 72 °C (1 min); four cycles of 95 °C (30 s), 55 °C (30 s) and 72 °C (1 min); four cycles of 95 °C (30 s), 56 °C (30 s) and 72 °C (1 min); and six cycles of 95 °C (30 s), 57 °C (30 s) and 72 °C (1 min). GenBank accession numbers, specimen voucher numbers and collection data are provided in the Table 1.

Sequence alignment and phylogenetic analysis

Sequence alignment

Sequence data were aligned and concatenated using Geneious R v.9.0.5 (Biomatters, http://www.geneious.com/). Protein-coding gene fragments (*CO1* and *CAD*) were aligned using MUSCLE (Edgar, 2004), and the ribosomal gene fragment (28S) was aligned using MAFFT v.7.017 (Katoh & Standley, 2013) with default settings (algorithm: Auto; scoring matrix: 200 PAM/k = 2; gap open penalty: 1.53; and offset value: 0.123). The reading frames of protein-coding gene fragments *CO1* and *CAD* were checked in Geneious R v.9.0.5 to ensure the absence of stop codons or other alignment problems.

Phylogenetic analyses

We performed analyses using three combinations of data: morphology only, molecular only and a third with both molecular and morphological datasets combined (total-evidence dataset). For the morphology-only dataset, we conducted an equal-weight maximum parsimony (MP) analysis in TNT v.1.5 (Goloboff & Catalano, 2016) using a New Technology Search with 10 000 trees held in memory, and 1000 parsimony ratchet iterations performed (Nixon, 1999), followed by 100 cycles of tree drifting and 100 rounds of tree fusing (Goloboff, 1999). Branch support was calculated with the bootstrap (BS, nona: 1000 replications, option 'mult*100; hold/100'). A BS ≥ 70 is considered as indicating strong support for a given node (Felsenstein, 1985).

For the molecular-only and total-evidence datasets, phylogenetic relationships were investigated using maximum likelihood (ML) and Bayesian inference (BI). Individual gene trees of each fragment were inferred with both ML and BI analyses (via analysis methods described below). The concatenated molecular dataset was partitioned a priori by codon position for protein-coding gene fragments (*CO1* and *CAD*), with the ribosomal gene fragment (28S) treated as a single whole partition, resulting in a total of seven partitions. Optimal partitioning schemes (Supporting Information, Table S2) and models for BI analyses were estimated with PartitionFinder v.2 (Lanfear *et al.*, 2016) using the '*greedy*' search algorithm, the '*MrBayes*' set of models, and the Bayesian information criteria (BIC) metric for model selection and scheme comparison; for ML analyses, we specified the partitions a priori and used the '*Auto*' function to find the best partitioning scheme (ModelFinder; Kalyaanamoorthy *et al.*, 2017) and using the in W-IQ-TREE v.1.5.4 (Nguyen *et al.*, 2015). For the total-evidence dataset, the morphological partition was

analysed using the MK model (Lewis, 2001) and run using MrBayes v.3.2.6 (Ronquist *et al.*, 2012).

The BI analyses were conducted in MrBayes v.3.2.6 (Ronquist *et al.*, 2012) using the BEAGLE library (Ayres *et al.*, 2012) on the CIPRES Science Gateway server (Miller *et al.*, 2010). We used two independent runs of eight Markov chain Monte Carlo (MCMC) chains (one cold and seven incrementally heated), each running for 20 million generations, with sampling every 1000 generations. After checking for convergence of the runs in Tracer v.1.5 (http://BEAST.bio.ed.ac.uk/Tracer) and applying a conservative burn-in of 25%, we used the command *sump* in MrBayes to calculate the posterior probabilities (PP) and *sumt* to produce a 50% majority rule consensus tree.

The ML analyses were carried out in IQ-TREE v.1.5.4 as implemented in W-IQ-TREE (http://iqtree.cibiv.univie.ac.at/; Trifinopoulos *et al.*, 2016). We performed 1000 ultrafast bootstrap replicates (UFBoot; Minh *et al.*, 2013) to investigate nodal support across topologies, using the SH-aLRT test (Guindon *et al.*, 2010). A posterior probability (PP) ≥ 0.95 and an UFBoot ≥ 95 were recognized as indicating strong support for a given node (Erixon *et al.*, 2003; Minh *et al.*, 2013).

Ancestral character state reconstruction

The analysis of morphological character evolution was conducted through ACSR with Mesquite v.3.10 (Maddison & Maddison, 2015) using the ML tree, because it offered a sounder hypothesis of the relationship between taxa (see 'Monophyly and systematic placement of Dorynotini within Cassidinae').

The MP approach was used to account for the incompleteness of sampling within the representatives of the tribe (Joy *et al.*, 2016). We reconstructed all 85 external anatomical characters and four internal anatomical characters, with a focus on the few characters that were used by previous authors to characterize different genera. The reconstructed characters states were as follows: antennal calli (absent; present, poorly developed; and present, well developed; character 28); shape of scutellum (triangular or diamond shaped; character 46); anterior margin of elytra with insertion pocket (character 49); shape of lateral margins (concave or convex/straight; character 53); presence of post-scutellar projection (character 56), and its shape (conical-shaped tubercle; triangular-shaped tubercle; and spiniform; character 57); angle formed at the base of pretarsal claws (obtuse; straight; acute; and subparallel with no angle near the base; character 82); and their symmetry (symmetrical; inconspicuously asymmetrical; and conspicuously asymmetrical; character 83).

RESULTS

Phylogenetic analyses

The concatenated molecular matrix comprised 2291 aligned base pairs. Analyses of the morphological dataset (MP) and the individual-gene and total-evidence datasets (under both ML and BI) produced topologies with low nodal support at nearly all nodes. All gene trees and total-evidence analyses recovered broadly similar phylogenetic patterns, with heterogeneous values of nodal support depending on the optimality criterion and dataset (see Supporting Information, Appendix S2, Figs S89–S96).

Both analyses (ML and BI) of the concatenated molecular dataset recovered Cassidini as the sister group to Dorynotini with strong support (UFBoot = 100, PP = 1.0). Cassidini is decisively paraphyletic, as previous phylogenetic reconstructions have demonstrated (Chaboo, 2007; López-Pérez *et al.*, 2017). A representative of Cassidini was recovered as sister taxon to Dorynotini in all analyses (Fig. 3), *Syngambria bisinuata* (Boheman, 1855) in the ML analysis and *Eremionycha bahiana* (Boheman, 1855) in the BI analysis (Fig. 4).

Dorynotini was strongly supported as monophyletic in all concatenated molecular analyses (UFBoot = 100, PP = 1.0). The genus *Paranota* was also recovered as monophyletic with strong support (UFBoot = 100, PP = 1.0), and the ML and BI topologies were congruent with respect to intrageneric phylogenetic relationships. The genus *Dorynota* was recovered as polyphyletic in all analyses (Fig. 4; Supporting Information, Appendix S2, Figs S89–S96), although there was some consistent structuring within the genus. The subgenus *Akantaka* was recovered as monophyletic with strong support (UFBoot = 99, PP = 0.98), albeit the intrasubgeneric phylogenetic relationships received low support and exhibited areas of conflict across analyses (Fig. 4). The subgenus *Dorynota s.s.* was recovered as paraphyletic with respect to other genera, with its members emerging in three different clades within the tree: (1) a strongly supported clade of South American *Dorynota s.s.* species ('clade 1'; UFBoot = 99, PP = 1.0) was recovered as sister to the rest of Dorynotini (UFBoot = 88, PP = 1.0); (2) *Dorynota* (*s.s.*) *aculeata*, was recovered as sister to *Paratrikona* (UFBoot = 97, PP = 0.87), together with *Omoteina* forming a clade endemic to the Greater Antilles, with high support ('clade 2'; UFBoot = 100, PP = 1.0); and (3) *Dorynota* (*s.s.*) *bidens* was recovered as sister to the subgenus *Akantaka*, with high support ('clade 3' UFBoot = 99, PP = 0.99) (Fig. 3).

The MP analysis of morphological data (Supporting Information, Appendix S2, Fig. S95) recovered a well-resolved strict consensus tree, collapsed from the

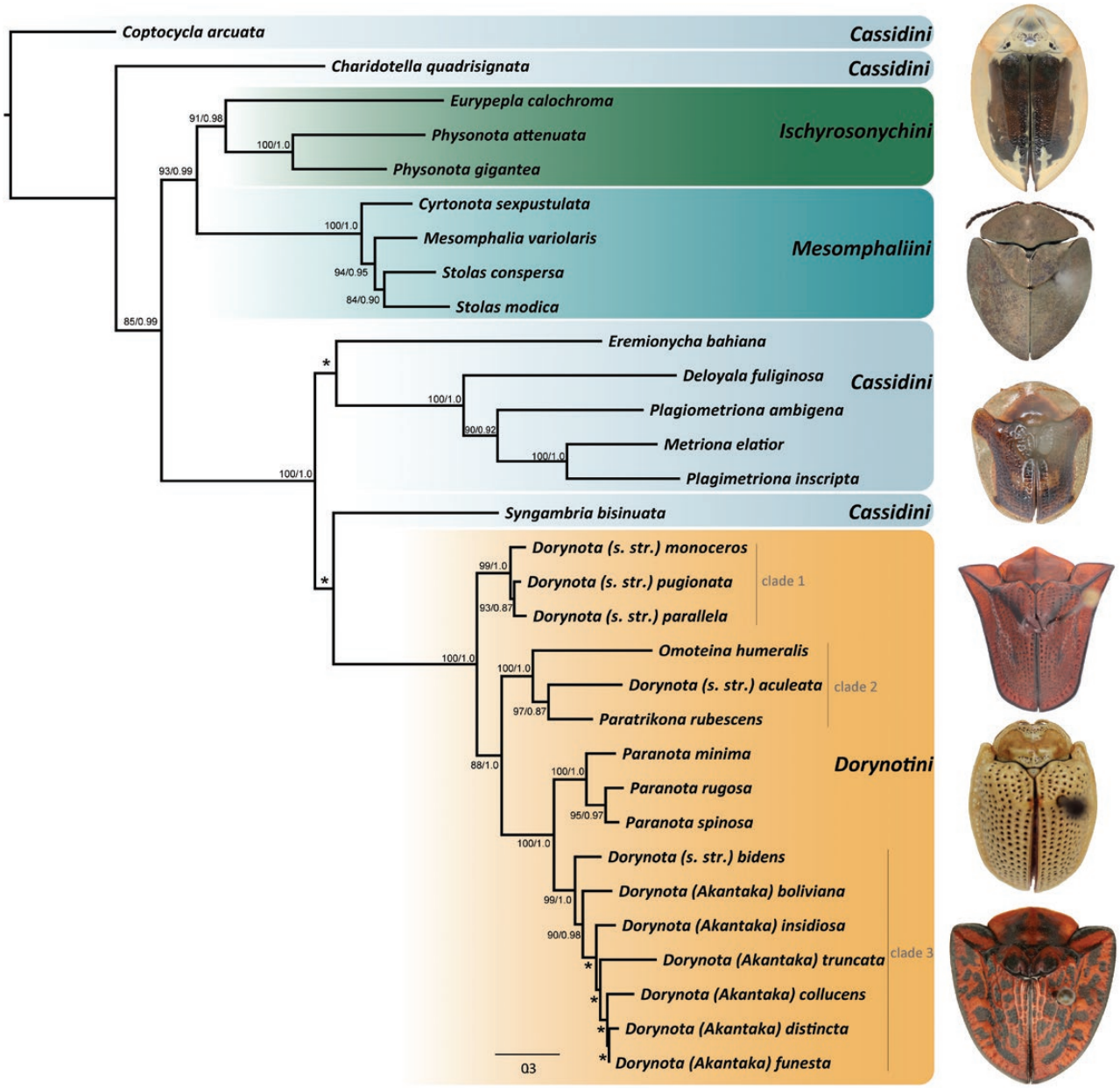

Figure 3. Phylogeny of the tribe Dorynotini based on maximum likelihood analysis of the concatenated molecular dataset comprising two nuclear (28S, *CAD*) and one mitochondrial (*CO1*) gene fragment. Nodal support values represent bootstraps of the maximum likelihood analysis and posterior probabilities of the Bayesian inference. Nodes that were not consistently recovered in all phylogenetic analyses are indicated by '*'. Adult Cassidinae photographs (top to bottom): *Physonota attenuata* Boheman; *Stolas modica* (Boheman); *Eremionycha bahiana* (Boheman); *Dorynota* (*s.s.*) *pugionata* (Germar); *Omoteina humeralis* (Olivier); and *Dorynota* (*Akantaka*) *truncata* (Fabricius).

16 shortest trees [length = 319, consistency index (CI) = 0.418, retention index (RI) = 0.752]. The topology recovered is congruent, in part, with results of the molecular dataset analyses. The tribe Dorynotini, the genus *Paranota* and subgenus *Akantaka* were recovered as monophyletic, with high nodal support (BS = 98, BS = 80 and BS = 49, respectively); and clades 2 and 3 were strongly supported (BS = 82 and BS = 80, respectively). *Dorynota s.s.* was recovered as paraphyletic, with representatives emerging independently in two clades along the tree: (1) within clade 2, with high nodal support (BS = 82); and (2) in a poorly supported clade (BS = 13), including the subgenera *Dorynota s.s.* and *Akantaka*, where *D.* (*s.s.*) *pugionata* and *D.* (*s.s.*)

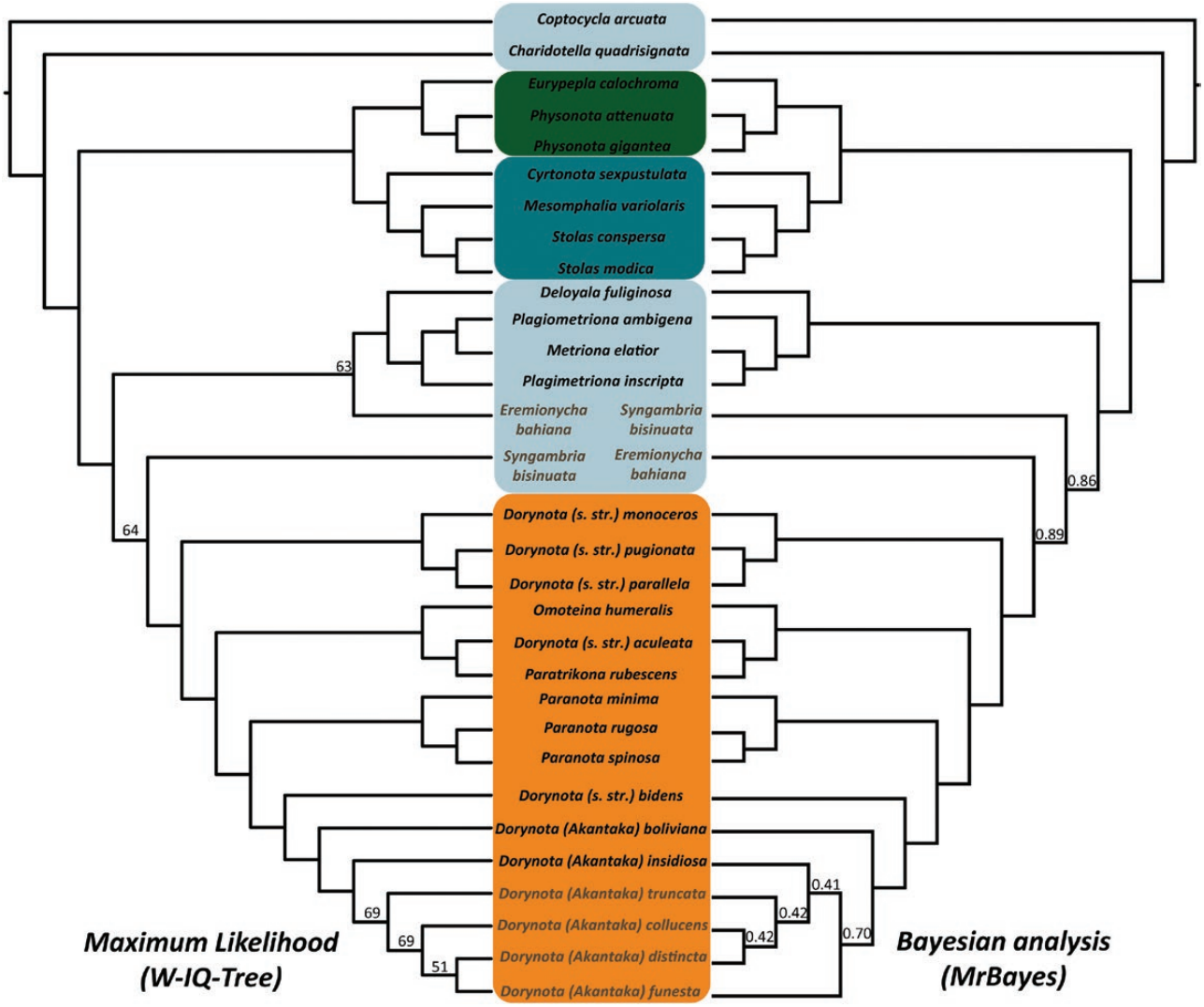

Figure 4. Mirrored topologies recovered using maximum likelihood (left) and Bayesian inference (right) analyses. Conflicting nodes between both analyses and respective nodal support values are depicted.

parallela are recovered as a clade, sister to *D.* (*s.s.*) *monoceros* and clade 3.

Ancestral character state reconstruction

For Dorynotini, the diamond-shaped scutellum (Supporting Information, Appendix S1, Figs S53, S54) and the spiniform post-scutellar projection (Supporting Information, Appendix S1, Figs S2, S52) were recovered as synapomorphies. The diamond-shaped scutellum exhibits a single reversal to triangular shaped (Supporting Information, Appendix S1, Figs S3, S51) in the Greater Antillean clade (Supporting Information, Appendix S1, Figs S3, S51), and the spiniform post-scutellar projection was lost in *Omoteina humeralis* and underwent transitions in *Paratrikona rubescens* and *Akantaka* to conical or triangular-shaped tubercles (Fig. 5A, B). The straight angle between the pretarsal claws was recovered as the plesiomorphic state within Dorynotini, which evolved to subparallel once in *Dorynota* (*s.s.*) *pugionata* + *Dorynota* (*s.s.*) *parallela*, and to an acute angle in the clades *Dorynota* (*s.s.*) *aculeata* + *Paratrikona rubescens* and *Paranota* (Supporting Information, Appendix S1, Figs S81–S83). Based on our results, the symmetry and angle at the base of the pretarsal claws are correlated characters within Dorynotini: subparallel claws are inconspicuously asymmetric, acute-angled base of claws are distinctly asymmetric, and obtuse-angled base of claws are symmetric (Fig. 5C). The presence of well-developed antennal calli was recovered as a synapomorphic character for the

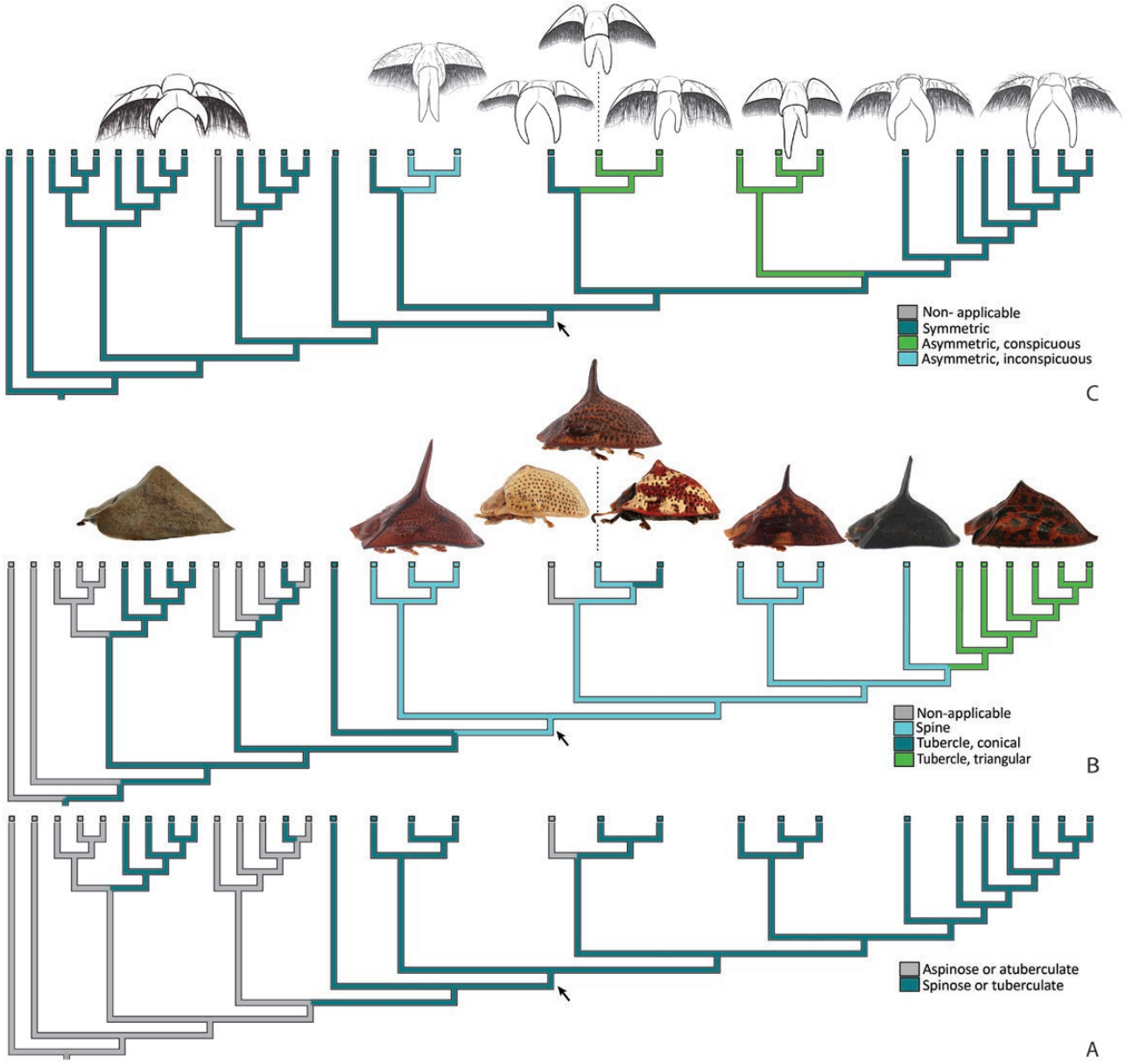

Figure 5. A–C, ancestral character state reconstruction (ACSR) of selective characters traditionally used to classify different genera of Dorynotini. The tribe stem node is indicated by an arrow. Branch colours highlight the results of the ACSR parsimony reconstruction. A, elytra dorsum with post-scutellar projection (character 56). B, shape of post-scutellar projection (character 57). C, symmetry of pretarsal claws (character 83). Adult Cassidinae species represented (left to right): *Stolas modica* (Boheman); *Dorynota* (*s.s.*) *pugionata* (Germar); *Omoteina humeralis* (Olivier); *Dorynota* (*s.s.*) *aculeata* (Boheman); *Paratrikona rubescens* Blake; *Paranota minima* (Wagener); *Dorynota* (*s.s.*) *bidens* (Fabricius); and *Dorynota* (*Akantaka*) *truncata* (Fabricius).

tribe, with one reversal to being poorly developed in *Paranota* + clade 3.

The ancestral character state reconstruction analysis also revealed other characters that appear to have a phylogenetic significance as potential synapomorphies for the tribe, which are as follows: w-shaped posterior angle of pronotum (character 25); the protibial apex depressed on the internal margin (character 40); presence of insertion pocket in the anterior margin of the elytra (character 49); presence of humeral ridge on the elytra (character 50); presence of locking system at the elytral suture (character 64);

epipleural ridge tooth (character 65); metasternum with elevated posterior margin (character 74); and protibial apex depressed on internal margin (character 40) (see Supporting Information, Appendix S3, Figs S98, S101, S104, S105, S109, S110, S113). The morphological characters traditionally used for diagnosing genera of the tribe were not recovered as synapomorphies but represent plesiomorphies or convergent characters. These characters include the scutellum shape, presence and shape of a post-scutellar spine/tubercle, and the disposition and asymmetry of the pretarsal claws.

Taxonomic classification

Clade 2 is consistently recovered as monophyletic in all analyses, with high nodal support (see Fig. 3; Supporting Information, Appendix S2, Figs S89–S96). It is composed of the three species endemic to the Greater Antilles: *O. humeralis*, *D.* (*s.s.*) *aculeata* and *P. rubescens*. Based on ACSR, this clade presents a general pattern of reversal of states considered plesiomorphic within Dorynotini. It is characterized by sharing the following character states: antennomere V wider at apex (character 8); pronotum with truncate posterior angle (character 25); absence of hypomeron depression (character 36); triangular-shaped scutellum (character 46); epipleural ridge tooth not conspicuously elevated (character 67); large, deep elytral punctuation (character 71); and metasternum strongly elevated (character 74) (see Supporting Information, Appendix S3, Figs S99, S100, S103, S111–S113).

To address the incongruence of the current classification with our results, we propose a nomenclatural reorganization of clade 2, by proposing the synonymy of the genus *Omoteina* with *Paratrikona* **syn. nov.**, and the transfer of its species and *D.* (*s.s.*) *aculeata* to the genus *Omoteina*. As a result, the clade is composed of ***Omoteina aculeata*** **(Boheman, 1854) comb. nov.,** ***Omoteina blakae*** **(Simões, 2017) comb. nov.,** ***Omoteina lerouxii*** **(Boheman, 1854) comb. nov.,** ***Omoteina ovata*** **(Blake, 1938) comb. nov.,** ***Omoteina rubescens*** **(Blake, 1939) comb. nov.,** ***Omoteina turrifera*** **(Boheman, 1854) comb. nov.,** ***Omoteina turritella*** **(Blake, 1837) comb. nov. and** ***Omoteina variegata*** **(Blake, 1939) comb. nov.**

For the remaining recovered clades, we do not propose any taxonomic changes. The Greater Antilles clade is the only clade that is consistently recovered with high support and presents a distributional pattern that offers another line of evidence supporting the clade as an independent lineage within Dorynotini.

DISCUSSION

Monophyly and systematic placement of Dorynotini in Cassidinae

Borowiec (1995) was the first to provide a cladistic test of the tribal relationships within the subfamily Cassidinae, based on 19 adult morphological characters that were previously used by Hincks (1952). In this seminal work, Borowiec (1995) recovered Dorynotini as part of a polytomy with the tribes Cassidini and Ischyrosonychini. However, he did not provide additional discussion on its placement or possible relationships with other tribes. Hsiao & Windsor (1999) used molecular data (12S mitochondrial DNA) to test the relationships between Hispinae and Cassidinae, but, only one species of Dorynotini was included, which was recovered as nested in Cassidini. Chaboo (2007) conducted a phylogenetic analysis of Cassidinae *s.l.*, based on morphological data of adults and immatures, including *Dorynota* and *Paratrikona*. Her analysis recovered Dorynotini + Ischyrosonychini as sister to Stolaini (= Mesomphaliini Chapuis, 1875). Lopez *et al.* (2017), based on 96 adult morphological characters, recovered the Dorynotini as sister to the Mesomphaliini + Cassidini *s.l.*, whereas in our results we recovered Cassidini as paraphyletic. In the present study, the two species recovered as sister to Dorynotini in the BI or ML analyses are currently placed within Cassidini: *Eremionycha bahiana* (Boheman, 1855) and *Syngambria bisinuata* (Boheman, 1855). Both species present different morphologies regarding the presence of the post-scutellar tubercle. Given the results of the parsimony ACSR on the ML tree, the most recent ancestor of Dorynotini had a cone-shaped tubercle post-scutellar projection (Fig. 5A, B), with the spiniform post-scutellar projection a synapomorphy for the tribe, secondarily lost in *O. humeralis* and convergently reduced to a tubercle in *P. rubescens* (cone shaped) and *Akantaka* (triangular shaped). *Syngambria bisinuata*, recovered as the sister taxon of Dorynotini in our ML analysis, has a conical tubercle post-scutellar projection, allowing for speculation on the transition to the elongate post-scutellar projection within the stem Dorynotini. In the BI analysis, *E. bahiana* is recovered as sister to Dorynotini and, although previously placed within the tribe, its morphology does not offer support for such a placement.

The w-shaped posterior angle of the pronotum varied from well marked to soft marked in our analysis. The shape of the posterior angle of the pronotum is generally associated with the presence of a diamond-shaped scutellum, a synapomorphy for the tribe, and the development of both characters is likely to be associated. The depressed internal margin of the protibia is possibly involved in antennal rubbing, as observed in

other groups of insects, where the foreleg rubs along the antenna in mid-air anterior or lateral to the head (Valentine, 1973). The presence of the insertion pocket in the anterior margin of the elytra helps to accommodate the pronotum, as the anterior margin of the elytra is expanded anteriorly and laterally, which also contributes to the formation of the conspicuous humeral angles. The locking system observed in the elytral suture could potentially be associated with the spiniform post-scutellar projection (synapomorphic for the tribe), because it is found in all dorynotine species but not in the outgroups. Monrós & Viana (1949) described the epipleural ridge tooth in the diagnosis of the genus *Dorynota*, '*dentículo elitral*' (= elytral tooth). In the present study, all members of Dorynotini present this character, varying from conspicuous to poorly conspicuous, and it could be another character contributing to the elytral locking mechanism. The elevated posterior margin of the metasternum is another feature that could potentially have a defensive function, facilitating the accommodation of retracted meso- and metalegs. The characters mentioned above need further examination to determine their adaptive function for members of the tribe.

Conflicts over morphological characters used for taxonomic classification in the tribe Dorynotini

Considering currently available evidence and based on our total-evidence approach, our results conflict with the morphological taxonomic system of Monrós & Viana (1949). This suggests that some morphological characters currently used for taxonomic classification are homoplastic and are therefore inapplicable for characterizing natural clades.

The genus *Paranota* and the subgenus *Akantaka* were recovered as monophyletic in our study. *Paranota* was characterized by having antennae with five glabrous basal antennomeres, six pubescent apical antennomeres, and asymmetric, parallel or subparallel pretarsal claws (Monrós & Viana, 1949). Simões (2014) compared the genus with the subgenus *Dorynota s.s.* and concluded that instead, *Paranota* should be characterized as presenting the following: slightly inserted pronotum in the internal margin of the anterior elytral angle; diamond-shaped scutellum; tarsomere IV slightly extending past III; and asymmetrical and subparallel claws. Based on our ACSR, we could not recover any of those characters as synapomorphies for the genus.

The subgenus *Akantaka* was described based on the presence of straight or convex lateral elytral margins and a triangular-shaped post-scutellar projection. Based on the ACSR, we recovered the triangular-shaped post-scutellar projection as a synapomorphy for the subgenus.

Omoteina (*sensu priori*), as a previously monotypic genus, was characterized by presenting gibbous elytra, deeply punctuate (Maulik, 1916), triangular scutellum and divergent symmetric claws (Monrós & Viana, 1949). Based on ACSR, the triangular-shaped scutellum was a reversal from the diamond shape found within Dorynotini, and symmetric claws are plesiomorphic in the tribe.

Species previously in *Paratrikona* (now in *Omoteina*, syn. nov.; **comb. nov.**) are rare in the field and in collections, usually known from short series of specimens (Simões, 2017). The genus is characterized by possessing elytra with coarse and regular punctuation and a short tubercle-like post-scutellar projection. Here, the genus is represented by a single species; therefore, its monophyly could not be tested. Results from the ACSR indicate that the coarse and regular punctuation are not diagnostic, but the tubercle post-scutellar projection is unique among Dorynotini and, based on our ACSR, it is a modification of the plesiomorphic spiniform post-scutellar projection found within the tribe.

The subgenus *Dorynota s.s.* was diagnosed by possessing a spiniform post-scutellar projection, the pronotum partly inserted in the elytral anterior margin, and subequal pretarsal claws (Monrós & Viana, 1949). In our analysis, we recover the subgenus *Dorynota s.s.* as paraphyletic, with representatives dispersed in three separate clades (Fig. 3). Clade 1 is recovered as sister to all other Dorynotini, grouping with a wide geographical range throughout central and southwest South America. The ancestral character state reconstruction did not recover potential synapomorphies for the clade. However, its internal sister taxa, *D.* (*s.s.*) *parallela* + *D.* (*s.s.*) *pugionata*, share two synapomorphies: mesoscutellum with transverse ridges poorly developed (character 44) (see Supporting Information, Appendix S3, Fig. S102), and parallel asymmetric pretarsal claws. Clade 2 is composed of species endemic to the Greater Antilles, *O. humeralis*, *D.* (*s.s.*) *aculeata* and *P. rubescens* (see 'Taxonomic classification' and discussion above). Clade 3 is composed of *D.* (*s.s.*) *bidens* recovered as sister to the subgenus *Akantaka*. Based on the ACSR, clade 3 shares many convergent characters with clade 1 (e.g. depressed surface of scutellum), and *D.* (*s.s.*) *bidens* and the subgenus *Akantaka* share characters that are plesiomorphic for the tribe (e.g. elevated posterior margin of metasternum). The lack of recovered synapomorphies for clade 3 highlights the need for further investigation of morphological characters and extended taxon sampling. However, it is noteworthy that *Akantaka* still forms a clade that is robustly delineated by an ambiguous synapomorphy, the triangular elytral post-scutellar projection.

The Greater Antillean clade

Besides the morphological characters previously cited (above), the Greater Antillean clade is also characterized by three of the four possible states of the post-scutellar projection among its representatives: absent, found in *O. humearlis*; conical-shaped tubercle, found in *O. rubescens* comb. nov. (transferred from *Paratrikona*); and spiniform, found in *O. aculeata* comb. nov. (transferred from *Dorynota*). Results of the ACSR indicate that the presence of the spine is the plesiomorphic state for all Dorynotini and was lost or transformed in two of the three lineages of the Greater Antilles clade.

Within clade 2, *O. aculeata* comb. nov. was recovered as the sister-species to *O. rubescens* comb. nov. Monrós & Viana (1949) previously suggested that these two species could be closely related based on the presence of the triangular-shaped scutellum, which was recovered here as a synapomorphic state of the whole Greater Antillean clade. Despite being incorrect with respect to this character, Monrós & Viana (1949) were correct about the cladistic relationship between the species, and our results based on the ancestral character state reconstruction recovered the pronotum with a rugose aspect as the synapomorphy for these species (character 18).

Another interesting feature observed among the members of the clade is the asymmetry in diversity between different morphotypes. Field observations and literature indicate that common species, found more easily in the field, present a well-developed spine (*O. aculeata* comb. nov.) or present no post-scutellar projection (*O. humeralis*), whereas species adorned with a short tubercle are more species rich but extremely rare and known only from short series of specimens (Blake, 1939; Borowiec, 2009; Simões, 2017). This asymmetry of diversification patterns, and morphological characters that might have shaped such patterns, should be investigated further with broader sampling of taxa.

Conclusions

This study represents the first attempt to investigate relationships within Dorynotini in a total-evidence phylogenetic framework. Here, we reaffirmed the reciprocal monophyly of the tribe Dorynotini, the genus *Paranota* and the subgenus *Akantaka*. However, with other dorynotine groups found to be para- or polyphyletic, our study shows that a revision of the classification of Dorynotini and a re-evaluation of the traditional morphological diagnostic characters are needed. The fact that almost all characters traditionally used for classifying genera in the tribe do not follow the pattern of natural groupings of the tribe indicate these necessities, and future investigations would thus strongly benefit from the guidance of molecular analyses. In this vein, we show that the presence of the post-scutellar spine, the most conspicuous character of Dorynotini, is a synapomorphy of the tribe and has been reduced and transformed in some of its lineages.

Our study offers substantial progress in resolving phylogenetic relationships among Dorynotini (and Cassidinae). Future work should focus on the addition of new morphological characters and increase the taxon and gene fragment sampling to improve our understanding of the systematics and evolution of tortoise beetles.

ACKNOWLEDGEMENTS

We thank the many curators and collection managers listed in the Supporting Information (Table S1) for allowing access to specimens at the respective institutions. We also thank the team that assisted with fieldwork in Brazil and the Dominican Republic: Antonio Tosto, Carlos De Soto Molinari, Claydson de Assis, Juan P. Botero, Mario Cupello and Rob van Brussel. We thank the students of the Entomology Division of the University of Kansas Natural History Museum for continued guidance and assistance; and A. Townsend Peterson, Jennifer Giron, Laura Breitkreuz, the editor and two anonymous reviewers for comments on an earlier version of the manuscript. Logistic support was provided by The Smithsonian Tropical Research Institute. M.V.P.S. received financial support from the Conselho Nacional de Desenvolvimento Científico e Tecnológico (CNPq; fellowship no. 201275/2012-0), from the following University of Kansas grants: Panorama Award; Division of Entomology; and Graduate Student Organization Award; and an Ernst Mayr Travel Grant provided by the Museum of Comparative Zoology (MCZ), Harvard University, and a Graduate Student Research Enhancement Award from the Coleopterists Society.

REFERENCES

Ayres DL, Darling A, Zwickl DJ, Beerli P, Holder MT, Lewis PO, Huelsenbeck JP, Ronquist F, Swofford DL, Cummings MP, Rambaut A, Suchard MA. 2012. BEAGLE: an application programming interface and high-performance computing library for statistical phylogenetics. *Systematic Biology* **61:** 170–173.

Baca SM, Toussaint EFA, Miller KB, Short AEZ. 2017. Molecular phylogeny of the aquatic beetle family Noteridae (Coleoptera: Adephaga) with an emphasis on data partitioning strategies. *Molecular Phylogenetics and Evolution* **107:** 282–292.

Blake DH. 1939. Eight new Chrysomelidae (Coleoptera) from the Dominican Republic. *Proceedings of the Entomological Society* **41:** 231–239.

Borowiec L. 1995. Tribal classification of the cassidoid Hispinae (Coleoptera: Chrysomelidae). In: Pakaluk J, Ślipiński SA, Crowson RA, eds. *Biology, phylogeny, and classification of Coleoptera: papers celebrating the 80th Birthday of Roy A. Crowson*. Warsaw: Muzeum i Instytut Zoologii PAN, 541–558.

Borowiec L. 1999. *A world catalogue of the Cassidinae (Coleoptera: Chrysomelidae)*. Wrocław: Biologica Silesiae.

Borowiec L. 2005. Three new species of the genus *Dorynota* sgen. *Akantaka* Maulik, 1916 from Bolivia and Brazil (Coleoptera: Chrysomelidae: Cassidinae: Dorynotini). *Genus* **16:** 29–41.

Borowiec L. 2009. New records of Neotropical tortoise beetles (Coleoptera: Chrysomelidae: Cassidinae). *Genus* **20:** 615–722.

Borowiec L, Świętojańska J. 2014. Cassidinae Gyllenhal, 1813. In: Leschen RAB, Beutel RG, eds. *Handbook of zoology: Coleoptera, beetles Volume 3: morphology and systematics (Phytophaga)*. Berlin/New York: deGruyter Press, 198–217.

Borowiec, L, Świętojańska J. 2018. *World catalog of Cassidinae*. Wrocław. Available at: http://www.cassidae.uni.wroc.pl/katalog%20internetowy/index.htm

Bouchard P, Bousquet Y, Davies AE, Alonso-Zarazaga MA, Lawrence JF, Lyal CHC, Newton AF, Reid CAM, Schmitt M, Ślipiński SA, Smith ABT. 2011. Family-group names in Coleoptera (Insecta). *ZooKeys* **88:** 1–972.

Chaboo CS. 2007. Biology and phylogeny of the Cassidinae Gyllenhal *sensu lato* (tortoise and leaf-mining beetles) (Coleoptera: Chrysomelidae). *Bulletin of the American Museum of Natural History* 1–250.

Crowson RA. 1938. The metendosternite in Coleoptera: a comparative study. *Transactions of the Royal Entomological Society of London* **87:** 397–415.

Dejean PFMA. 1836. *Catalogue des Coléoptères de la collection de M. le Comte Dejean. [Livraison 5]*. Paris: Méquignon-Marvis.

Edgar RC. 2004. MUSCLE: multiple sequence alignment with high accuracy and high throughput. *Nucleic Acids Research* **32:** 1792–1797.

Erixon P, Svennblad B, Britton T, Oxelman B. 2003. Reliability of Bayesian posterior probabilities and bootstrap frequencies in phylogenetics. *Systematic Biology* **52:** 665–673.

Felsenstein J. 1985. Confidence limits on phylogenies: an approach using the bootstrap. *Evolution* **39:** 783–791.

Goloboff P. 1999. Analyzing large data sets in reasonable times: solutions for composite optima. *Cladistics* **15:** 415–428.

Goloboff PA, Catalano SA. 2016. TNT version 1.5, including a full implementation of phylogenetic morphometrics. *Cladistics* **32:** 221–238.

Guindon S, Dufayard JF, Lefort V, Anisimova M, Hordijk W, Gascuel O. 2010. New algorithms and methods to estimate maximum-likelihood phylogenies: assessing the performance of PhyML 3.0. *Systematic Biology* **59:** 307–321.

Hincks WD. 1952. The genera of the Cassidinae (Coleoptera: Chrysomelidae). *Transactions of the Royal Entomological Society of London* **103:** 327–358.

Hsiao TH, Windsor DM. 1999. Historical and biological relationships among Hispinae inferred from 12S mtDNA sequence data. In: Cox ML, ed. *Advances in Chrysomelidae biology 1*. Leiden: Backhuys, 39–50.

Hübler N, Klass KD. 2013. The morphology of the metendosternite and the anterior abdominal venter in Chrysomelinae (Insecta: Coleoptera: Chrysomelidae). *Arthropod Systematics and Phylogeny* **71:** 3–41.

Joy JB, Liang RH, McCloskey RM, Nguyen T, Poon AF. 2016. Ancestral reconstruction. *PLoS Computational Biology* **12:** e1004763.

Kalyaanamoorthy S, Minh BQ, Wong TKF, von Haeseler A, Jermiin LS. 2017. ModelFinder: fast model selection for accurate phylogenetic estimates. *Nature Methods* **14:** 587–589.

Katoh K, Standley DM. 2013. MAFFT multiple sequence alignment software version 7: improvements in performance and usability. *Molecular Biology and Evolution* **30:** 772–780.

Lanfear R, Frandsen PB, Wright AM, Senfeld T, Calcott B. 2016. PartitionFinder 2: new methods for selecting partitioned models of evolution for molecular and morphological phylogenetic analyses. *Molecular Biology and Evolution* **34:** 772–773.

Lewis PO. 2001. A likelihood approach to estimating phylogeny from discrete morphological character data. *Systematic Biology* **50:** 913–925.

López-Pérez S, Zaragoza-Caballero S, Ochoterena H, Morrone JJ. 2017. A phylogenetic study of the worldwide tribe Cassidini Gyllenhal, 1813 (Coleoptera: Chrysomelidae: Cassidinae) based on morphological data. *Systematic Entomology* **1813:** 1–15.

Maddison WP, Maddison DR. 2015. *Mesquite: a modular system for evolutionary analysis*. *Version 3.04*. Available at: http://mesquiteproject.org

Maulik S. 1916. On Cryptostome beetles in the Cambridge University Museum of Zoology. *Journal of Zoology* **86:** 567–589.

Miller MA, Pfeiffer W, Schwartz T. 2010. Creating the CIPRES Science Gateway for inference of large phylogenetic trees. *2010 Gateway Computing Environments Workshop, GCE 2010*.

Minh BQ, Nguyen MA, von Haeseler A. 2013. Ultrafast approximation for phylogenetic bootstrap. *Molecular Biology and Evolution* **30:** 1188–1195.

Monrós F, Viana MJ. 1949. Revision de las especies Argentines de Dorynotyni (Col. Cassidae). *Acta Zoologica Lilloana* **8:** 391–426.

Nguyen LT, Schmidt HA, von Haeseler A, Minh BQ. 2015. IQ-TREE: a fast and effective stochastic algorithm for estimating maximum-likelihood phylogenies. *Molecular Biology and Evolution* **32:** 268–274.

Nixon K. 1999. The parsimony ratchet, a new method for rapid parsimony analysis. *Cladistics* **15:** 407–414.

Ronquist F, Teslenko M, van der Mark P, Ayres DL, Darling A, Höhna S, Larget B, Liu L, Suchard MA, Huelsenbeck JP. 2012. MrBayes 3.2: efficient Bayesian phylogenetic inference and model choice across a large model space. *Systematic Biology* **61:** 539–542.

Simões MVP. 2014. Taxonomic revision of the genus *Paranota* Monrós and Viana, 1949 (Coleoptera: Chrysomelidae: Cassidinae: Dorynotini). *The Coleopterists Bulletin* **68:** 631–655.

Simões MVP. 2017. Revision of the Greater Antilles genus *Paratrikona* Spaeth, 1923 (Coleoptera: Chrysomelidae: Cassidinae: Dorynotini). *Zootaxa* **4238:** 417–425.

Simões MVP, Lieberman BS, Soberón J, Peterson AT. 2017. Testing environmental correlates of clines in clades: an example from cassidine beetles. *Insect Conservation and Diversity* **10:** 472–482.

Simões MVP, Sekerka L. 2014. Redescription of *Heteronychocassis acuticollis* Spaeth, 1915 (Coleoptera: Chrysomelidae: Cassidinae). *The Coleopterists Bulletin* **68:** 407–410.

Simões MVP, Sekerka L. 2015. Review of the neotropical leaf beetle subgenus *Dorynota s.s.* Chevrolat (Coleoptera: Chrysomelidae: Cassidinae: Dorynotini). *The Coleopterists Bulletin* **69:** 231–254.

Simon C, Frati F, Beckenbach A, Crespi B, Liu H, Flook P. 1994. Evolution, weighting, and phylogenetic utility of mitochondrial gene sequences and a compilation of conserved polymerase chain reaction primers. *Annals of the Entomological Society of America* **87:** 651–701.

Spaeth F. 1923. Ueber Batonota Hope (Col. cassid). *Wiener entomologische Zeitung* **40:** 65–76.

Suzuki K. 1994. Comparative morphology of the hindwing venation of the Chrysomelidae (Coleoptera). In: Jolivet PH, Cox ML, Petitpierre E. eds. *Novel aspects of the biology of Chrysomelidae*. Series Entomologica, vol 50. Dordrecht: Springer, 337–354.

Trifinopoulos J, Nguyen LT, von Haeseler A, Minh BQ. 2016. W-IQ-TREE: a fast online phylogenetic tool for maximum likelihood analysis. *Nucleic Acids Research* **44:** W232–W235.

Valentine BD. 1973. Grooming behavior in Coleoptera. *The Coleopterists Bulletin* **27:** 63–73.

Van der Auwera G, Chapelle S, De Wachter R. 1994. Structure of the large ribosomal subunit RNA of *Phytophthora megasperma*, and phylogeny of the oomycetes. *FEBS Letters* **338:** 133–136.

Wild AL, Maddison DR. 2008. Evaluating nuclear protein-coding genes for phylogenetic utility in beetles. *Molecular Phylogenetics and Evolution* **48:** 877–891.

SUPPORTING INFORMATION

Additional Supporting Information may be found in the online version of this article at the publisher's web-site:

Table S1. Material examined for coding morphological characters.
Table S2. Optimal partitioning schemes and models for Bayesian inference analyses estimated with PartitionFinder.
Appendix S1. Morphological data.
Appendix S2. Figures of resulting gene trees and total-evidence analysis.
Appendix S3. Figures of ancestral character state reconstruction.